Acta Materialia 166 (2019) 424–434

Contents lists available at ScienceDirect

Acta Materialia

journal homepage: www.elsevier.com/locate/actamat

Full length article

The effect of randomness on the strength of high-entropy alloys

Luchan Zhang [a, b], Yang Xiang [a, *], Jian Han [b], David J. Srolovitz [c, b, d, **]

[a] Department of Mathematics, The Hong Kong University of Science and Technology, Clear Water Bay, Kowloon, Hong Kong
[b] Department of Materials Science and Engineering, University of Pennsylvania, Philadelphia, PA 19004, USA
[c] Department of Materials Science and Engineering, City University of Hong Kong, Kowloon, Hong Kong
[d] Department of Mechanical Engineering and Applied Mechanics, University of Pennsylvania, Philadelphia, PA 19004, USA

ARTICLE INFO

Article history:
Received 14 July 2018
Received in revised form
14 December 2018
Accepted 17 December 2018
Available online 27 December 2018

Keywords:
High-entropy alloys
Dislocations
Materials strength
Peierls-nabarro model

ABSTRACT

High-entropy alloys (HEAs), i.e., single-phase, (nearly) equiatomic multicomponent, metallic materials, are associated with novel mechanical properties, such as high strength, fracture resistance etc. In this paper, a stochastic Peierls-Nabarro (PN) model is proposed to understand how random site occupancy affects intrinsic strength. The stochastic PN model accounts for the randomness in the composition, characterized by both the standard deviation of the perturbation in the interplanar potential and the correlation length within the spatial compositional distribution. The model presented includes the effects of non-uniform compositional distribution both in the direction of dislocation glide and along a dislocation line to predict overall dislocation glide resistance. The model predicts the intrinsic strength of HEAs as a function of the standard deviation and the correlation length of the randomness. We find that, in most of the parameter space, the compositional randomness in an HEA gives rise to an intrinsic strength that far exceeds that of any of the pure metals from which the HEA is composed. This approach provides a fundamental explanation to the origin of the high strength of HEAs.

1. Introduction

High-entropy alloys (HEAs) are often described as single-phase, (nearly) random solid solutions of four or more elements of (nearly) equal composition [1–3]. The crystal structures of such HEAs are often very simple; e.g., face-centered or body-centered cubic crystals. HEAs exhibit useful and novel mechanical properties [4], fracture resistance [5], corrosion resistance [6], and radiation damage resistance [7]. The mechanical property profile is characterized by a combination of high strength, high ductility and high fracture toughness [2,5]; hence, HEAs have attracted considerable interest for potential applications as structural materials. HEA design (composition and microstructure) will rely on establishing the link between structure and mechanical performance. In this paper, we examine such a linkage at a fundamental level; in particular, what are the implications of atomic-level randomness on dislocation glide in HEAs.

Many of the existing models for the strength of HEAs are based on the classical ideas of solute solution strengthening; e.g., the Labusch model [8]. The original Labusch model asserts that the critical shear stress for dislocation glide may be described as $\sigma_c \sim f^{4/3}c^{2/3}$, where c is the concentration of solute atoms and f is the interaction force between a solute atom and a dislocation. While the original Labusch model is directly applicable for cases where there is a distinction between solute and solvent atoms (unlike in HEAs), extensions to the HEA case have focused on how to combine contributions from each component to the strength by defining f_n and c_n for the n^{th} element [9–11]. For example, Toda-Caraballo et al. [10] adopted an averaging procedure in which $\sigma_c \sim (\sum_n f_n^2 c_n)^{2/3}$. Varvenne et al. [12,13] explicitly considered the interaction energy between a solute atom and a dislocation in a matrix that was described as an effective medium composed of all of the other types of atoms; such solute strengthening models were parameterized consistent with atomistic simulation results [14]. Their model leads to a Labusch-type of expression for the strength: $\sigma_c \sim [\sum_{\mathbf{r},n} f_n^2(\mathbf{r})c_n]^{2/3}$, where $\mathbf{r}$ denotes the position of a solute atom in the effective matrix relative to a dislocation.

In our view, there are two main issues with classical solid solution approaches. First, the interaction between a solute atom and a dislocation based on elastic interactions associated with atomic size misfit and modulus misfit of the solute atom (with respect to the matrix) does not explicitly account for the interaction between solute atoms and the dislocation core. Such effects are particularly

* Corresponding author.
** Corresponding author. Department of Materials Science and Engineering, University of Pennsylvania, Philadelphia, PA 19004 USA.
E-mail addresses: maxiang@ust.hk (Y. Xiang), srol@seas.upenn.edu (D.J. Srolovitz).

https://doi.org/10.1016/j.actamat.2018.12.032
1359-6454/

important, because in concentrated solutions the solute concentration near the core may be very large and these interactions are sensitive to the nature of the atomic bonding in the core. The importance of local bonding details in dislocation cores plays a major role in the mechanical response in a wide-range of materials and crystal structures [15]. Because of the atomic-scale randomness associated with HEAs, the local distortion around each atom is very localized. Hence, we suggest that the local bonding effects at the dislocation core may, in many cases, be at least as important as the elastic interactions.

Second, while HEAs are solid solutions, we expect that the distribution of elements is not completely random; i.e., there is chemical short-range order (SRO). While SRO is difficult to measure experimentally, the existence of SRO in HEAs was reported based on direct atomistic simulations [16–20]. SRO is known to increase alloy strength. Indeed, motion of dislocations through a solute solution with SRO disturbs the local order and produces additional resistance for dislocation glide, as suggested by Fisher [21] and confirmed experimentally [22,23]. SRO may also affect the temperature dependence of the yield stress. Unlike in pure face-centered cubic (FCC) metals, FCC HEAs exhibit strongly temperature dependent yield stresses [4,24]. Otto et al. [24] attributed this to thermally activated dislocation motion associated with short-range obstacles (barriers). The short-range obstacles may correspond to local regions of large SRO. Although SRO influences the mechanical properties of HEAs, SRO is not included in the HEA solute strengthening models.

Our paper has two main goals: (1) to understand the effects of distributed solutes on dislocation cores and how they move, and (2) to consider the effect of the random nature of this solute distribution (and its spatial correlations). We examine these effects generically, so that they can be used in a wide variety of contexts and as additional effects to those already well-known models. We emphasize that this paper is not a complete description of all effects that solutes have on dislocations nor is it focused on the specific distribution of solutes in any particular concentrated alloy.

More specifically, we present a model for the influence of the randomness in the spatial distribution of composition on the strength of HEAs that naturally describes dislocation core effects in a generic manner; i.e., based upon a Peierls-Nabarro (PN) dislocation model [25,26]. While such a model is not an accurate description of the true complexity of dislocation cores, it does provide a heuristic description of dislocation core effects that may be generalized to describe the influence of SRO. In the PN model, the disregistry across the glide plane is explicitly considered, and an interplanar potential is used to model the local effect of chemical bonding in the dislocation core. The distribution of chemical components can also be included by making the interplanar potential spatially varying in a purely random manner or with SRO. We first introduce the classical PN model and then extend it to form a random, stochastic PN model. Next, we consider the effect of SRO by making this random variation in composition spatially variable with a well-defined correlation length. Finally, we extend our approach beyond the one-dimensional PN model to describe dislocation motion on a two-dimensional slip plane and add some simplistic applications to HEAs.

2. The classical Peierls-Nabarro model

The Peierls-Nabarro (PN) model is a continuum model that combines a long-range description of the strain field of a dislocation and an atomic-level description of its core. In its classical form, it describes a straight edge dislocation [25–27] with its core spread over a finite region along the slip plane. We assume that the dislocation line is located along the z-axis, its Burgers vector is parallel to the x-axis, and x-z is the slip plane. The (flat) slip plane separates two linear elastic, continuum half-spaces ($y>0$ and $y<0$). The disregistry across the slip plane (i.e., slip in the x-direction) may be described by the function $\phi(x)$; $\phi(x\rightarrow-\infty)\rightarrow 0$ and $\phi(x\rightarrow+\infty)\rightarrow b$, where b is the magnitude of the Burgers vector. The Burgers vector distribution is $\rho(x)=\phi'(x)$; this distribution characterizes the dislocation core in this model.

The total energy of a dislocation in the PN model may be written as

$$E_{\text{total}} = E_{\text{elastic}} + E_{\text{misfit}}, \tag{1}$$

where E_{elastic} is the elastic energy in the upper and lower half spaces delimited by the slip plane and E_{misfit} is the misfit energy associated with the nonlinear (atomic) interactions across the slip plane. The elastic energy is a function of the disregistry distribution:

$$E_{\text{elastic}} = \frac{1}{2}\int_{-\infty}^{+\infty}\sigma_{xy}(x)\phi(x)dx, \tag{2}$$

where the shear stress across the slip plane may be written in terms of the disregistry $\sigma_{xy}(x)=\frac{\mu}{2\pi(1-\nu)}\int_{-\infty}^{+\infty}\frac{\phi'(x_1)}{x-x_1}dx_1$ (μ and ν are the shear modulus and Poisson ratio). The misfit energy may also be written in terms of the disregistry:

$$E_{\text{misfit}} = \int_{-\infty}^{+\infty}\gamma(\phi(x))dx, \tag{3}$$

where $\gamma(\phi)$ is the periodic, interplanar potential (generalized stacking-fault energy). In the classical PN model, $\gamma(\phi)$ is approximated by the Frenkel sinusoidal potential [27,28],

$$\gamma(\phi) = \frac{\mu b^2}{4\pi^2 d}\left(1-\cos\frac{2\pi\phi}{b}\right), \tag{4}$$

where d is the atomic interplanar spacing perpendicular to the slip plane.

Equilibrium is obtained by minimizing the total energy with respect to the disregistry distribution: $\delta E_{\text{total}}/\delta\phi = 0$. The equilibrium disregistry function is

$$\phi(x) = \frac{b}{\pi}\tan^{-1}\left(\frac{x}{\zeta_0}\right)+\frac{b}{2}, \tag{5}$$

where ζ_0 is the dislocation core width:

$$\zeta_0 = \frac{d}{2(1-\nu)}. \tag{6}$$

There is energetic barrier that must be overcome to move the dislocation along the slip plane. The energy barrier and the critical stress for doing so are known as Peierls barrier and Peierls stress, respectively. In the PN model, the Peierls barrier and stress for the Frenkel interplanar potential are $E_{\text{p}}^0=\mu b^2/[\pi(1-\nu)]\exp(-2\pi\zeta_0/b)$ and

$$\sigma_{\text{p}}^0 = \frac{\mu}{1-\nu}\exp\left(-\frac{2\pi\zeta_0}{b}\right); \tag{7}$$

both are functions of the ratio of dislocation core width to Burgers vector ζ_0/b. In our numerical calculations below, we will assume $d=b$ and $\nu=0.347$.

3. Stochastic Peierls-Nabarro model: uniform randomness

In a high-entropy alloy (HEA), the local environment varies with location in the lattice because the material is a solid solution of many elements. However, unlike a random dilute binary alloy, where most of the lattice sites are occupied by atoms of a single type (only a minority of sites are occupied by atoms of another type), in an HEA, the local site occupancies vary from site to site on an atomic scale. Hence, a dilute binary alloy model is inappropriate for describing HEAs. Here, we extend the PN to describe the randomness in the elemental site occupancies of an HEA as a random variation in the amplitude of the interplanar potential. This, in turn, leads to stochastic variations in the dislocation core width, Peierls stress, and Peierls energy and, as we demonstrate later, significantly alters the yield strength of the material.

Specifically, we incorporate randomness into the PN model to describe an HEA, by scaling the interlayer potential (Eq. (4)) with a random variable ω; i.e.,

$$E_{\text{misfit}} = \int_{-\infty}^{+\infty} \omega(x)\gamma(\phi(x))dx \approx \omega \int_{-\infty}^{+\infty} \gamma(\phi(x))dx. \tag{8}$$

Since this randomness is allowed to vary from position to position along the slip plane $\omega(x)$, the first expression can account for random variation on any scale. In other words, $\omega(x)$ may account for any short-range order that may occur in the HEA (i.e., spatial, chemical short-range correlations). In the second expression, however, we replace the actual variation along the slip plane by considering an ensemble of models, each with a spatially uniform interlayer potential whose amplitude determined by the random x-independent variable ω (i.e., infinite spatial correlation). This is the uniform randomness case which is the focus of this section. We return to consider the first (i.e., spatial short-range correlation) case in the next section. For each case, we examine the dislocation core width, the Peierls stress, and the distance a dislocation may travel under a fixed, applied stress in the HEA.

We assume that the random variable ω is described by a probability density function $P_\omega(u)$ (in this notation, u refers to a particular value of the random variable ω). The cumulative probability density function associated with P_ω is $F_\omega(u) = \int_0^u P_\omega(v)dv$.

Incorporating the randomness in the interlayer potential leaves the elastic energy unchanged except for a rescaling of the misfit energy by a factor of ω. Following the solution of the equilibrium disregistry function in Eq. (5), we assume that, with the random-amplitude interlayer potential, the equilibrium disregistry function that describes the dislocation core still takes the form

$$\phi(x) = \frac{b}{\pi}\tan^{-1}\left(\frac{x}{\zeta}\right) + \frac{b}{2}. \tag{9}$$

The equilibrium dislocation core width ζ is determined from $dE_{\text{total}}/d\zeta = -\mu b^2/[4\pi(1-\nu)\zeta] + \mu b^2\omega/2\pi d = 0$:

$$\zeta = \frac{d}{2(1-\nu)\omega} = \frac{\zeta_0}{\omega}, \tag{10}$$

where ζ_0 is the core width in the classical PN model (Eq. (6)). The core width, relative to that in the uniform system, is $\tilde{\zeta} = \zeta/\zeta_0 = 1/\omega$ (see Eq. (10)). The probability distribution for the core width $P_{\tilde{\zeta}}(u)$ is related to the probability distribution P_ω of ω as

$$P_{\tilde{\zeta}}(u) = \left(\frac{1}{u}\right)^2 P_\omega\left(\frac{1}{u}\right). \tag{11}$$

Accordingly, the cumulative distribution for the core width $F_{\tilde{\zeta}}(u)$ is related to that for the random variable ω as $F_{\tilde{\zeta}}(u) = 1 - F_\omega(1/u)$.

We consider that the random variable ω is described by a normal/Gaussian distribution with mean 1 and standard deviation Δ, i.e., its probability function is

$$P_\omega(u;1,\Delta) = \frac{1}{\Delta\sqrt{2\pi}} e^{-\frac{(u-1)^2}{2\Delta^2}}. \tag{12}$$

In the mathematical literature, this normal distribution is often written as $\omega \sim \mathcal{N}(1,\Delta)$; a notation we adopt below. The mean value 1 implies that the averaged value of the interlayer potential at each site on the slip plane of the HEA equals that of the lattice with a single-type atom, as in Eq. (4). The probability distribution of the (normalized) dislocation core size $\tilde{\zeta}$ (using Eq. (11) with ω following this normal distribution) for several values of Δ is shown in Fig. 1. The mean core size and its standard deviation are tabulated in the inset to that figure for the value of Δ. These results demonstrate that, when $\Delta = 0$, the probability density of $\tilde{\zeta}$ is a delta function, which corresponds to the classical PN model core width. As Δ increases, the most probable core width (peak of the distribution) gets smaller and the core width distribution broadens. However, the mean value $\langle\tilde{\zeta}\rangle$ and standard deviation $\Delta_{\tilde{\zeta}}$ of the core width both increase with increasing Δ. This means that, as the standard deviation of the randomness of the interplanar potential amplitude increases, the most probable dislocation core width decreases, whereas the mean value of the dislocation core width increases.

A small aside regarding the assumption that the randomness is characterized by a normal distribution (Eq. (12)) is in order. This distribution was chosen for its flexibility, that it is well-known, and because it is simpler to use than many other possible choices. However, it is an undesirable characteristic that this distribution has a finite probability for $\omega < 0$; this is unphysical. We have examined the effect that this has on several dislocation properties by comparing predictions using the normal distribution to that obtained using the Gamma distribution with the same mean and standard deviation (this distribution is finite only for $\omega > 0$). The results are shown in Supplemental Material. Comparisons show that the results using the normal distribution are good approximations to those using the Gamma distribution.

The randomness in the interlayer potential also makes the Peierls stress a distributed quantity. Using the misfit energy with the random interplanar potential in Eq. (8) and the disregistry function in Eq. (9) and following the standard procedure of lattice summation of the misfit energy in the classical PN model, we determine the Peierls stress: $\sigma_p^* = \omega\mu/(1-\nu)\exp(-2\pi\zeta/b)$. Unfortunately, the probability density function of σ_p^* cannot be solved analytically from that of the random variable ω. Instead, we look for

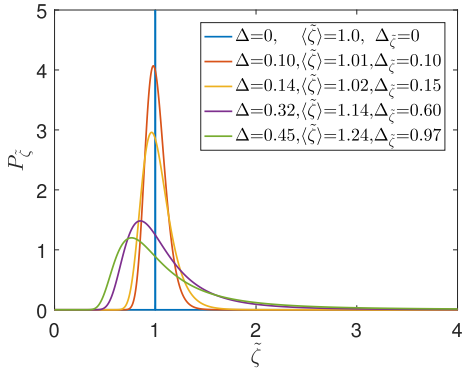

Fig. 1. The (normalized) dislocation core width $\tilde{\zeta}$ distribution for several values of Δ for normally distributed ω, i.e., $\mathcal{N}(1,\Delta)$. The inset to the figures shows the mean $\langle\tilde{\zeta}\rangle$ and standard deviation $\Delta_{\tilde{\zeta}}$ of the core width.

a reasonable approximation for the Peierls stress that yields analytical forms of the probability density function. Noting that the Peierls stress σ_p^* is sensitive to the dislocation core width ζ, we keep the exponential term in σ_p^* and approximate ω in its factor by its mean value 1. As shown in the Supplemental Material, this is a good approximation for the physically reasonable case where the standard deviation of ω is small compared with its mean value 1. This leads to the following approximate formula of the Peierls stress in the HEA: $\sigma_p = \mu/(1-\nu)\exp(-2\pi\zeta/b)$, or the reduced Peierls stress:

$$\tilde{\sigma}_p = \sigma_p \Big/ \sigma_p^0 = \exp\Big(\beta^{-1}\Big(1-\omega^{-1}\Big)\Big), \tag{13}$$

where $\beta = b/2\pi\zeta_0$.

The probability distribution for the normalized Peierls stress $\tilde{\sigma}_p$ is $P_{\tilde{\sigma}_p}(u) = P_\omega(1/(1-\beta\log u))(\beta/u)(1-\beta\log u)^{-2}$. This probability density function is shown in Fig. 2 for several values of Δ, along with its mean $\langle\tilde{\sigma}_p\rangle$ and standard deviation $\Delta_{\tilde{\sigma}_p}$. For $\Delta = 0$, the probability distribution of $\tilde{\sigma}_p$ is a delta function and we recover the classical Peierls stress. With increasing Δ, the most probable Peierls stress (peak in the probability density function) shifts towards smaller $\tilde{\sigma}_p$ and the distribution widens. For sufficiently large Δ, however, the probability distribution of $\tilde{\sigma}_p$ becomes monotonically decreasing (narrowing with increasing $\tilde{\sigma}_p$). The mean value $\langle\tilde{\sigma}_p\rangle$ and standard deviation $\Delta_{\tilde{\sigma}_p}$ of the Peierls stress, on the other hand, increase with increasing Δ for all Δ. This means that as the standard deviation of the randomness of the interplanar potential amplitude increases, the most probable Peierls stress decreases, whereas the mean value of the Peierls stress increases.

When a stress is applied to the HEA σ_a ($\tilde{\sigma}_a \equiv \sigma_a/\sigma_p^0$), a dislocation will glide until the local Peierls stress σ_p is too large to overcome at the applied stress. The probability that a dislocation will be able to move past any particular atomic site is $P(\tilde{\sigma}_p < \tilde{\sigma}_a) = F_{\tilde{\sigma}_p}(\tilde{\sigma}_a) = F_\omega(1/[1-\beta\log(\tilde{\sigma}_a)])$. Hence, the probability that the dislocation will be able to travel a distance $D = Nb$ before it meets a barrier that it is unable to overcome is $P_D(N;\tilde{\sigma}_a) = P^N(\tilde{\sigma}_p < \tilde{\sigma}_a)P(\tilde{\sigma}_p > \tilde{\sigma}_a) = F_\omega^N(1/[1-\beta\log(\tilde{\sigma}_a)])(1-F_\omega(1/[1-\beta\log(\tilde{\sigma}_a)]))$. This implies that the mean distance $\overline{D}$ a dislocation moves under an applied stress is

$$\overline{D} = \sum_N NbP_D(N;\tilde{\sigma}_a) = b\sum_N NF_\omega^N(q)[1-F_\omega(q)], \tag{14}$$

where $q \equiv 1/[1-\beta\log(\tilde{\sigma}_a)]$. This is valid in the physically meaningful regime where $\sigma_a < \mu/(1-\nu)$ (or $\tilde{\sigma}_a < e^{1/\beta}$).

Fig. 3(a) shows the mean distance a dislocation moves under an applied stress for several values of Δ. When $\Delta = 0$, the mean distance a dislocation can travel is either zero ($\sigma_a < \sigma_p^0$) or infinite ($\sigma_a \geq \sigma_p^0$). Importantly, when the width of the distribution of ω is finite ($\Delta > 0$), the dislocation will only be able to travel a finite distance for any applied stress. Fig. 3(b) shows the distribution of distances that a dislocation will travel for several applied stresses. This is not surprising, since a moving dislocation has a finite probability of encountering a local Peierls stress that is above the applied stress. The mean distance a dislocation can move increases exponentially with applied stress. Fig. 3(a) can also be examined in terms of what stress must be applied in order to move a dislocation the same distance. Clearly, the stress required to move a dislocation any non-trivial distance increases rapidly with increasing randomness Δ. These results imply that the randomness that characterizes HEAs will have a profound effect on the yield behavior of the material (see below).

4. Stochastic Peierls-Nabarro model: short-range correlations

A high-entropy alloy is never completely random. The fact that atomic interactions depend on atom type (element) implies that, at any finite temperature, the enthalpy of mixing is non-zero. This implies that some degree of short-range order (SRO) will always be present and any particular atom type will have either an enhanced or reduced probability for neighboring atoms to have particular atom types. While this is a thermodynamic effect, kinetics associated with synthesis or processing may alter the degree of SRO that occurs.

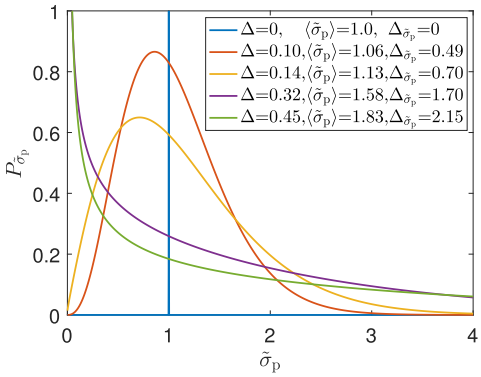

Fig. 2. The probability distribution function of the Peierls stress $\tilde{\sigma}_p$ for several values of Δ, where ω is normally distributed. The inset shows its mean $\langle\tilde{\sigma}_p\rangle$ and standard deviations $\Delta_{\tilde{\sigma}_p}$ for each Δ.

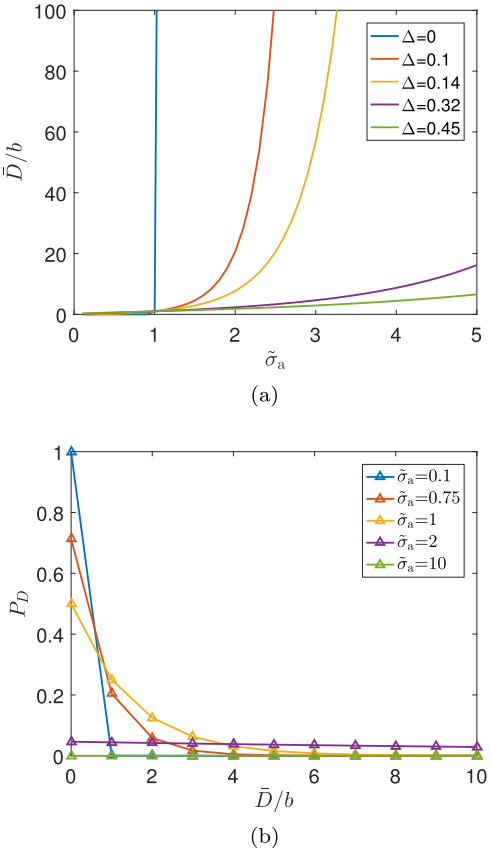

Fig. 3. (a) The mean distance $\overline{D}$ a dislocation will move in an HEA as a function of the applied stress $\tilde{\sigma}_a$ for several values of Δ. (b) The probability distribution for this distance $P_D(N;\tilde{\sigma}_a)$ for several applied stresses. Note that when the applied stress is large ($\tilde{\sigma}_a = 10$), the dislocation traveling a long distance is (almost) equally probable as traveling a short distance. As a result, the probability for the dislocation to stop at each specific place (at any distance) is small (this is a result of the normalization of the probability).

The existence of SRO in HEAs suggests that a moving dislocation will not see a truly random distribution of neighboring environments. In this section, we propose an approach to incorporate spatial correlation of environments on dislocation motion. To this end, we return to the general form of the misfit energy in the Peierls-Nabarro model; i.e., the first expression in Eq. (8) for the interplanar potential. That is, we replace the classical, sinusoidal Frenkel interplanar potential $\gamma(\phi(x))$ (Eq. (4)) with $\omega(x)\gamma(\phi(x))$, where $\omega(x)$ is a stochastic coefficient function with short-range spatial correlation. Formally, we describe $\omega(x)$ as a stationary Gauss-Markov process [29,30]. In particular, this is done through application of the Ornstein-Uhlenbeck process [29–31] which is a widely applied, nontrivial form of this process and which satisfies the stochastic differential equation

$$d\omega(x) = \frac{1-\omega(x)}{\lambda}dx + \sqrt{\frac{2}{\lambda}}\Delta dW_x, \tag{15}$$

where λ is the spatial range of the correlation or the correlation length of the random perturbation $\omega(x)$ over the space, Δ is the standard deviation of $\omega(x)$ at each lattice site (as before), and W_x is a continuous-time stochastic process that leads to Brownian motion (i.e., the Wiener process [32]). The expectation of $\omega(x)$ remains $\langle\omega(x)\rangle = 1$, such that, in the absence of the stochastic effect, the misfit energy in Eq. (8) reduces to the deterministic formula in Eq. (3).

The stochastic coefficient function $\omega(x)$ can be determined from Eq. (15) as

$$\omega(x) = 1 + \sqrt{\frac{2}{\lambda}}\Delta\int_{-\infty}^{x}\exp\left(-\frac{x-s}{\lambda}\right)dW_s. \tag{16}$$

The values of $\omega(x)$ at two different lattice sites, x_1 and x_2, are correlated as

$$\Big\langle(\omega(x_1)-1)(\omega(x_2)-1)\Big\rangle = \Delta^2\exp\left(-\frac{|x_1-x_2|}{\lambda}\right). \tag{17}$$

This means that λ is the correlation length of the random perturbation over the space. In other words, spatial correlations in the composition decay exponentially with separation between atomic sites with a decay distance of λ. Fig. 4 shows $\omega(x)$ for several different values of λ at fixed Δ. When the correlation length $\lambda\to 0$, $\langle(\omega(x_1)-1)(\omega(x_2)-1)\rangle\to 0$, which indicates that the randomness at x_1 and x_2 are independent of each other. When $\lambda\to\infty$, the variance $\langle[\omega(x_1)-\omega(x_2)]^2\rangle\to 0$, and therefore $\omega(x_1) = \omega(x_2)$; this is the case of uniform randomness considered in Section 3.

We now examine the effect of spatially correlated randomness on dislocation properties, beginning with the dislocation core width ζ. As in the previous section, we assume that the equilibrium disregistry function $\phi(x)$ that describes the dislocation core still takes the form in Eq. (9). Recall that the equilibrium dislocation core width ζ is that which minimizes the total energy $dE_{\text{total}}/d\zeta = 0$. The misfit energy is (see Eqs. (8), (9) and (16))

$$E_{\text{misfit}} = \frac{\mu b^2\zeta}{2\pi d} + \frac{\mu b^2}{4\pi^2 d}\sqrt{\frac{2}{\lambda}}\Delta\int_{-\infty}^{+\infty}\int_{-\infty}^{x}\exp\left(-\frac{x-s}{\lambda}\right)dW_s\frac{2\zeta^2}{x^2+\zeta^2}dx, \tag{18}$$

and the elastic energy is as per Eq. (2). For $\Delta\ll 1$, the dislocation core width $\tilde{\zeta} = \zeta/\zeta_0$ can be expressed as a function of λ as

$$\frac{1}{\tilde{\zeta}} = 1 + \frac{2\zeta_0}{\pi}\sqrt{\frac{2}{\lambda}}\Delta\int_{-\infty}^{+\infty}\int_{s}^{\infty}\exp\left(-\frac{x-s}{\lambda}\right)\frac{x^2}{\left(x^2+\zeta_0^2\right)^2}dxdW_s. \tag{19}$$

$1/\tilde{\zeta}$ follows a normal distribution with mean 1 and standard deviation

$$\overline{\Delta} = \frac{2\zeta_0}{\pi}\sqrt{\frac{2}{\lambda}}\Delta\sqrt{\int_{-\infty}^{+\infty}\left[\int_{s}^{+\infty}\exp\left(-\frac{x-s}{\lambda}\right)\frac{x^2}{\left(x^2+\zeta_0^2\right)^2}dx\right]^2 ds}, \tag{20}$$

i.e.,

$$\frac{1}{\tilde{\zeta}} \sim \mathcal{N}\left(1,\overline{\Delta}\right). \tag{21}$$

More details are provided in the Supplemental Material.

Fig. 5 shows the dislocation core width $\tilde{\zeta}$ distribution for different values of λ and Δ. These results are also tabulated in Table 1. As $\Delta\to 0$ and/or $\lambda\to 0$, we recover the classical Peierls-Nabarro prediction for the dislocation core width. With the increase of Δ at fixed λ, $\tilde{\zeta}$ distribution broadens and the peak shifts to smaller core size. More interestingly, increasing correlation length λ at fixed Δ leads to broadening of the core width $\tilde{\zeta}$ distribution. As $\lambda\to\infty$, we recover the uniform randomness results from the previous section.

We now examine the effect of spatial correlations in the composition ($\omega(x)$) in the HEA on the Peierls stress. As discussed in Section 3, it is reasonable to approximate the Peierls stress distribution based on the assumption that it is controlled by the randomness in the dislocation core width following Eq. (7). This yields

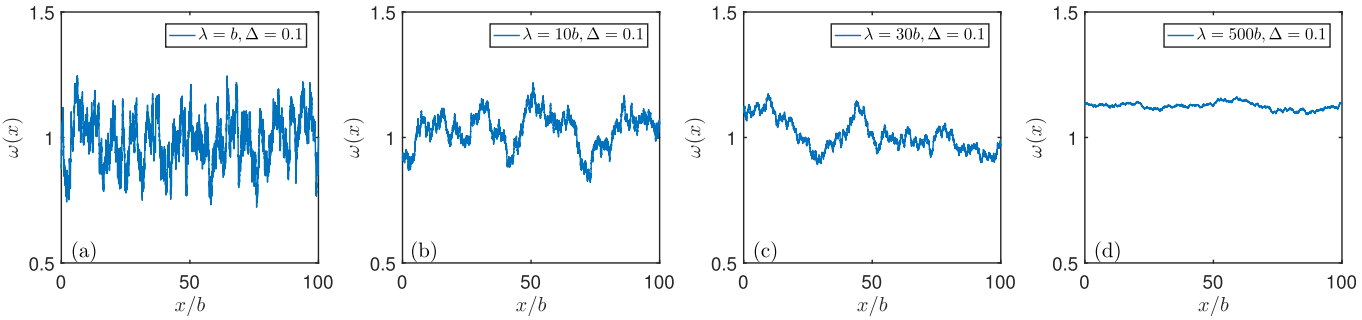

Fig. 4. The random coefficient function $\omega(x)$ defined by the Ornstein-Uhlenbeck process for several different values of the spatial correlation length λ at $\Delta = 0.1$. Although the mean value of $\omega(x)$ appears to be greater than one in (d), over a very large distance ($x\gg\lambda$) the average will be unity.

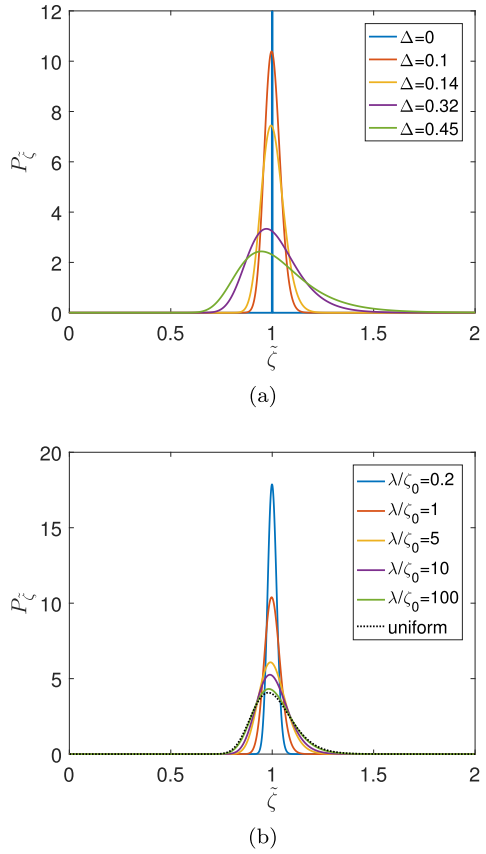

Fig. 5. The dislocation core width $\tilde{\zeta}$ distribution with spatially correlated random coefficient function $\omega(x)$ (a) for different values of Δ at $\lambda/\zeta_0 = 1$ and (b) for different values of λ/ζ_0 at $\Delta = 0.1$.

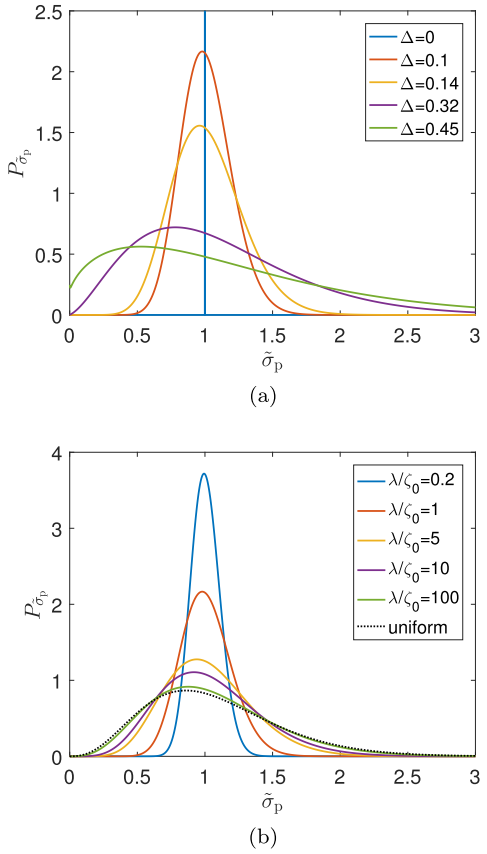

Fig. 6. The Peierls stress $\tilde{\sigma}_p$ distributions for the case of spatially correlated random coefficient function $\omega(x)$ are shown in (a) for several values of Δ at $\lambda/\zeta_0 = 1.0$ and in (b) for several values of λ/ζ_0 at $\Delta = 0.1$.

$$\tilde{\sigma}_p = \exp\left[\beta^{-1}\left(1-\tilde{\zeta}\right)\right], \tag{22}$$

where dislocation core width $\tilde{\zeta}$ is as per Eq. (19), and $1/\tilde{\zeta}$ is described by a normal distribution given by Eqs. (20) and (21).

Fig. 6 shows the probability density function of the Peierls stress $\tilde{\sigma}_p$ for several values of Δ and λ/ζ_0. The associated mean $\langle\tilde{\sigma}_p\rangle$ and standard deviation $\Delta_{\tilde{\sigma}_p}$ of the Peierls stress $\tilde{\sigma}_p$ distribution are summarized in Table 2. Increasing Δ at fixed λ leads to increasing mean Peierls stress, a shift in the most probably Peierls barrier to lower values and an increase in the width of the Peierls stress distribution. Increasing the spatial correlation length λ at fixed Δ leads to increasing mean Peierls stress, small shifts in the most probably Peierls barrier to lower values and a broadening of the Peierls stress distribution. Consistent with the dislocation core width $\tilde{\zeta}$ results, as $\Delta \to 0$ and/or $\lambda \to 0$, the Peierls stress goes to its classical Peierls-Nabarro value and as $\lambda \to \infty$ the Peierls stress distribution goes to the uniform randomness limit, as discussed above.

We now consider how a dislocation moves in an HEA with spatially correlated atomic site occupancies under an applied stress $\tilde{\sigma}_a = \sigma_a/\sigma_p^0$, following the same approach as in the previous section. The probability that a dislocation can move a distance $D = Nb$

Table 1
The mean value $\langle\tilde{\zeta}\rangle$ and standard deviation $\Delta_{\tilde{\zeta}}$ of the core width $\tilde{\zeta}$ for several values of Δ and λ/ζ_0.

λ/ζ_0	Δ	0	0.10	0.14	0.32	0.45
0.2	$\langle\tilde{\zeta}\rangle$	1.0	1.0	1.0	1.01	1.01
	$\Delta_{\tilde{\zeta}}$	0	0.02	0.03	0.07	0.10
1	$\langle\tilde{\zeta}\rangle$	1.0	1.0	1.0	1.02	1.03
	$\Delta_{\tilde{\zeta}}$	0	0.04	0.05	0.13	0.20
5	$\langle\tilde{\zeta}\rangle$	1.0	1.0	1.01	1.05	1.12
	$\Delta_{\tilde{\zeta}}$	0	0.07	0.10	0.27	0.53
10	$\langle\tilde{\zeta}\rangle$	1.0	1.01	1.01	1.07	1.17
	$\Delta_{\tilde{\zeta}}$	0	0.08	0.11	0.36	0.69
100	$\langle\tilde{\zeta}\rangle$	1.0	1.01	1.02	1.11	1.21
	$\Delta_{\tilde{\zeta}}$	0	0.09	0.13	0.47	0.84
∞ (uniform)	$\langle\tilde{\zeta}\rangle$	1.0	1.01	1.02	1.14	1.24
	$\Delta_{\tilde{\zeta}}$	0	0.10	0.15	0.60	0.97

Table 2
The mean value $\langle\tilde{\sigma}_p\rangle$ and standard deviation $\Delta_{\tilde{\sigma}_p}$ of the Peierls stress $\tilde{\sigma}_p$ for several values of Δ and λ/ζ_0.

λ/ζ_0	Δ	0	0.10	0.14	0.32	0.45
0.2	$\langle\tilde{\sigma}_p\rangle$	1.0	1.0	1.01	1.03	1.07
	$\Delta_{\tilde{\sigma}_p}$	0	0.11	0.15	0.35	0.50
1.0	$\langle\tilde{\sigma}_p\rangle$	1.0	1.01	1.02	1.10	1.19
	$\Delta_{\tilde{\sigma}_p}$	0	0.19	0.26	0.61	0.88
5	$\langle\tilde{\sigma}_p\rangle$	1.0	1.03	1.06	1.28	1.52
	$\Delta_{\tilde{\sigma}_p}$	0	0.32	0.45	1.10	1.59
10	$\langle\tilde{\sigma}_p\rangle$	1.0	1.04	1.08	1.37	1.64
	$\Delta_{\tilde{\sigma}_p}$	0	0.37	0.53	1.29	1.81
100	$\langle\tilde{\sigma}_p\rangle$	1.0	1.06	1.11	1.53	1.80
	$\Delta_{\tilde{\sigma}_p}$	0	0.46	0.66	1.60	2.09
∞ (uniform)	$\langle\tilde{\sigma}_p\rangle$	1.0	1.06	1.13	1.58	1.83
	$\Delta_{\tilde{\sigma}_p}$	0	0.49	0.70	1.70	2.15

under an applied stress $\tilde{\sigma}_a$ is $P_D(N;\tilde{\sigma}_a) = F^N_{\mathcal{N}(1,\overline{\Delta})}(1/(1-\beta\log\tilde{\sigma}_a))[1-F_{\mathcal{N}(1,\overline{\Delta})}(1/(1-\beta\log\tilde{\sigma}_a))]$. From this, we calculate the mean distance a dislocation moves $\overline{D}$ under applied stress $\tilde{\sigma}_a$:

$$\overline{D} = b\sum_N NF^N_{\mathcal{N}(1,\overline{\Delta})}\left(\frac{1}{1-\beta\log(\tilde{\sigma}_a)}\right)\left(1-F_{\mathcal{N}(1,\overline{\Delta})}\left(\frac{1}{1-\beta\log(\tilde{\sigma}_a)}\right)\right). \tag{23}$$

Note that in the correlated randomness case, $1/\tilde{\zeta}$ is described by the normal distribution $\mathcal{N}(1,\overline{\Delta})$, instead of $\mathcal{N}(1,\Delta)$ as in the uniform randomness case (previous section).

Fig. 7 shows the mean distance a dislocation moves $\overline{D}$ under applied stress $\tilde{\sigma}_a$ in the spatially correlated random composition ($\omega(x)$) case for several values of Δ and λ. $\overline{D}(\tilde{\sigma}_a)$ exhibits a similar variation with Δ for the spatially correlated and uniform randomness case, Fig. 3(a); i.e., for any finite Δ, the dislocation travels a finite distance at any applied stress, and as the applied stress $\tilde{\sigma}_a$ increases, $\overline{D}$ increases exponentially (when $\Delta = 0$ the dislocation will either not move or move infinitely far). The stress that must be applied to move a dislocation the same distance increases with increasing Δ. More interestingly for the present discussion, increasing the spatial correlation length λ implies either that the dislocation travels a shorter distance for a fixed applied stress or that greater applied stresses are required to move the dislocation a fixed distance. In the limit that the correlation length $\lambda/\zeta_0 \to \infty$, the results converge to the uniform random case, Fig. 3(a), as expected.

In general, increasing correlation length λ interpolates the dislocation properties between that of the non-random case (classical Peierls-Nabarro prediction) to the uniform randomness case (of the previous section).

5. Homogenized stochastic model

While the stochastic model with correlated randomness provide a useful approach to understanding the effects of randomness on dislocation motion in HEAs, it would be convenient to recast the model in such a way that ω is no longer a function of position. That is, instead of making the approximation that led to the second expression in Eq. (8), we would like to have a homogenized model that accounts for spatial correlation in the randomness without assuming that the randomness is uniform. To this end, we rewrite the misfit energy as

$$E_{\text{misfit}} = \overline{\omega}\int_{-\infty}^{+\infty}\gamma(\phi(x))dx. \tag{24}$$

We can do this by choosing a $\overline{\omega}$ as a random variable described by the normal distribution:

$$\overline{\omega} \sim \mathcal{N}\left(1,\overline{\Delta}\right), \tag{25}$$

where the standard deviation $\overline{\Delta}$ is given by Eq. (20), which explicitly depends on both λ and Δ.

In fact, by using this homogenized model in Eq. (24), the dislocation core width $\tilde{\zeta}$ is given by Eq. (10), i.e., $1/\tilde{\zeta} = \overline{\omega}$. We can see that it is the same as the full stochastic model result in Eq. (21) if Eq. (25) holds. That is, the random dislocation core widths in the two models following the same distribution. As a result, the Peierls stresses and the distance a dislocation moves calculated from the dislocation core widths are also the same using the two models. In this sense, we conclude that the model in Eqs. (24) and (25) represent a homogenized version of the fully stochastic model presented in the previous section.

The relation between the standard deviation $\overline{\Delta}$ of the random variable $\overline{\omega}$ and the spatial correlation length λ of $\omega(x)$ is shown in Fig. 8. We see that the standard deviation $\overline{\Delta}$ of the random variable $\overline{\omega}$ scales in a nonlinear but monotonic manner with the spatial correlation length λ. When $\lambda \to 0$, the standard deviation $\overline{\Delta} \to 0$, which corresponds to the classical Peierls-Nabarro model; when $\lambda \to \infty$, the standard deviation $\overline{\Delta} \to \Delta$, which corresponds to the uniform randomness case in Section 3. This is consistent with the discussion at the beginning of Section 4. The standard deviation $\overline{\Delta}$ of the random variable $\overline{\omega}$ is linearly dependent on the parameter Δ, which is the standard deviation of $\omega(x)$ at each location x.

6. Peierls stress in two dimensions

The model presented is one-dimensional and should be viewed in the same manner as the classical Peierls-Nabarro model. One limitation of focusing on one dimension is that dislocation motion can be completely stopped by a Peierls barrier at one atomic site. Of course, in a two-dimensional slip plane, a dislocation can bow around an obstacle that it cannot cross. Here, we make use of the one-dimensional model to provide insight into the strength of local barriers and use it as input to a simple two-dimensional model.

Consider a dislocation line in two dimensions. Along the dislocation line, the Peierls stress at each lattice site may be approximated by Eq. (22) following the one dimensional stochastic model in Section 4. This stochastic model may be represented by a random variable $\overline{\omega}$ as discussed in Section 5, and the associated Peierls stress may be approximated by $\tilde{\sigma}_p = \exp[\beta^{-1}(1-\overline{\omega}^{-1})]$, where $\overline{\omega} \sim \mathcal{N}(1,\overline{\Delta})$ and the standard deviation $\overline{\Delta}$ is as per Eq. (20).

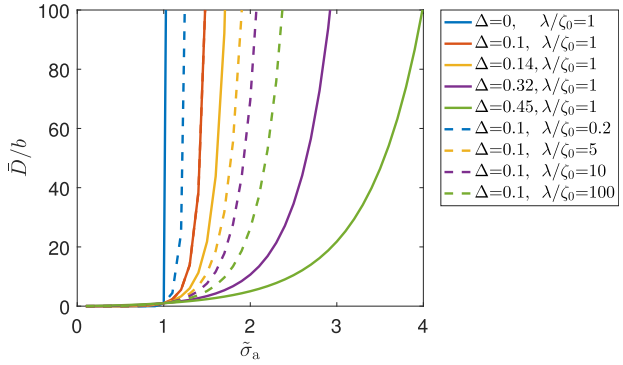

Fig. 7. Under applied stress $\tilde{\sigma}_a$, the mean value $\overline{D}$ of the dislocation traveled distance in a HEA with spatially correlated random coefficient function $\omega(x)$ with several different values of Δ and λ.

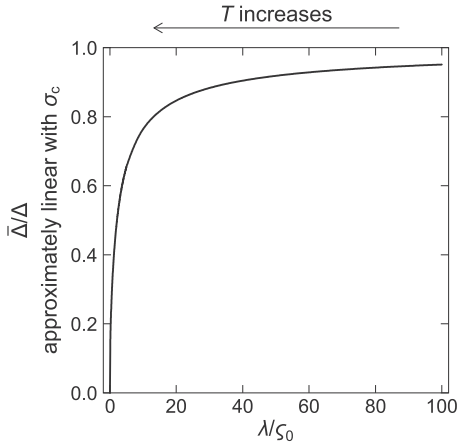

Fig. 8. The standard deviation $\overline{\Delta}$ of the random variable $\overline{\omega}$ as a function of the spatial correlation length λ of $\omega(x)$.

We now consider the ability of a dislocation to bow around obstacles, in the Orowan-looping sense [33]. The critical (Orowan) stress for a dislocation to bypass a set of "pinning sites" is

$$\sigma_c = \mu b/L, \tag{26}$$

where L is the average spacing between the pinning sites. Along the dislocation line, the ratio of the number of pinning lattice sites to that of the total sites is approximately $P(\tilde{\sigma}_p > \tilde{\sigma}_c)$, that is,

$$P(\tilde{\sigma}_p > \tilde{\sigma}_c) = a_0/L, \tag{27}$$

where $\tilde{\sigma}_c \equiv \sigma_c/\sigma_p^0$ and a_0 is the lattice constant ($b \approx a_0$). The critical stress, therefore, must satisfy the condition (using Eqs. (26) and (27)):

$$\frac{\sigma_p^0}{\mu}\tilde{\sigma}_c = P(\tilde{\sigma}_p > \tilde{\sigma}_c). \tag{28}$$

This probability can be written as $P(\tilde{\sigma}_p > \tilde{\sigma}_c) = 1 - F_{\mathcal{N}(1,\overline{\Delta})}(1 - \beta \log \tilde{\sigma}_c)$. Further using $1 - F_{\mathcal{N}(1,\overline{\Delta})}(u) = \frac{1}{2}\mathrm{erfc}\left(\frac{1}{\sqrt{2\overline{\Delta}}}(u^{-1} - 1)\right)$, the equation for the critical stress Eq. (28) becomes

$$\frac{2\sigma_p^0}{\mu}\tilde{\sigma}_c = \mathrm{erfc}\left[\frac{1}{\sqrt{2\overline{\Delta}}}\left(\frac{1}{1 - \beta \log \tilde{\sigma}_c} - 1\right)\right]. \tag{29}$$

Now, we simplify Eq. (29) for the case where the critical stress σ_c is close to the Peierls stress σ_p^0 (i.e., $\tilde{\sigma}_c \sim 1$). When $\tilde{\sigma}_c = 1$, the left-hand-side of Eq. (29) is $2\sigma_p^0/\mu$. Let z_0 be the value that satisfies $2\sigma_p^0/\mu = \mathrm{erfc}(z_0)$. Approximating the error function as $\mathrm{erfc}(z) \approx \mathrm{erfc}(z_0) + \frac{d}{dz}\mathrm{erfc}(z_0)(z - z_0)$ in Eq. (29) for $z_0 \equiv \mathrm{erfc}^{-1}(2\sigma_p^0/\mu)$, we find that

$$\frac{2\sigma_p^0}{\mu}\tilde{\sigma}_c \approx \frac{2\sigma_p^0}{\mu} - \frac{2\exp(-z_0^2)}{\sqrt{\pi}}\left[\frac{1}{\sqrt{2\overline{\Delta}}}\beta(\tilde{\sigma}_c - 1) - z_0\right] \tag{30}$$

or

$$\tilde{\sigma}_c = 1 + \frac{\frac{2z_0\exp(-z_0^2)}{\sqrt{\pi}}}{\frac{2\sigma_p^0}{\mu} + \frac{\sqrt{2}\beta\exp(-z_0^2)}{\sqrt{\pi}\overline{\Delta}}} \approx 1 + \frac{2\sqrt{2}\pi z_0\zeta_0}{b}\overline{\Delta}. \tag{31}$$

This approximation is valid for small $\overline{\Delta}$. Recall that $\overline{\Delta}$ is the standard deviation of the effective random variable $\overline{\omega}$, Eq. (20), and depends on the correlation length λ and the standard deviation Δ at each location of the random coefficient function $\omega(x)$.

The critical stress $\tilde{\sigma}_c$ determined by using the analytical approximation in Eq. (31) is shown in Fig. 9 along with those obtained by numerically solving the full equation in Eq. (29). Clearly, the approximation (Eq. (31)) provides a good approximation to the critical stress $\tilde{\sigma}_c$ for small Δ. These results demonstrate that the dimensionless critical stress $\tilde{\sigma}_c$ increases linearly with the standard deviation of the randomness Δ at each lattice, and increases monotonically (but nonlinearly) with the correlation length λ (see Fig. 8).

The critical stress σ_c is the yield strength increment associated with randomness in the spatial distribution of the elements in the HEA. This strengthening arises from the interaction between the dislocation core and the locally varying atomic-level environment.

7. Discussion

Our approach to describing strengthening in high-entropy alloys is fundamentally different from strengthening models based upon Fleischer [34] or Labusch [8] types of solute strengthening. While

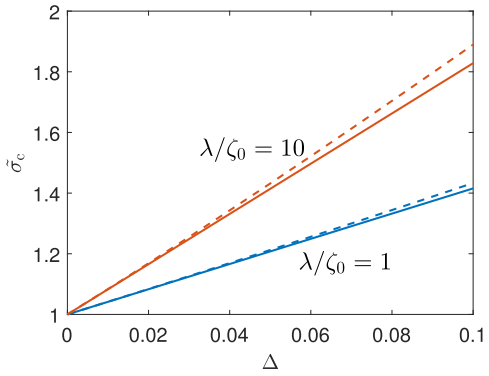

Fig. 9. The critical stress $\tilde{\sigma_c}$ determined using the analytical approximation in Eq. (31) (solid lines) and by numerical solution of the full equation in Eq. (29) (dashed lines), as functions of Δ for two different correlation lengths, λ/ζ_0.

solute strengthening models consider some atoms as solvents and others as solute, such distinctions are unclear in HEAs where there is no nominal solvent since most HEAs consist of many elements in near equiatomic concentrations. Varvenne et al. [13] proposed using an "average alloy" reference with properties (e.g., elastic constants) chosen/fit to match the HEA. In a concentrated alloy, local interactions between solute atoms screens the long-range elastic interactions between any particular solute and the dislocation core. Hence, short range solute/dislocation core interactions are more important in HEAs than in dilute solid solutions. At small length scales, it is not possible to separate these solute/dislocation elastic interactions from dislocation core effects. A complete description should, of course, fully account for the details of the dislocation cores and the subtlety of bonding in the highly distorted core region. Models based on standard solute strengthening approaches cannot account for such core effects. Our approach focuses on dislocation core effects within the idealized (and relatively simple) framework of the Peierls-Nabarro model which includes explicit core effects (including non-linear elastic deformation in the core).

We estimate the core strengthening effect in an HEA based on the PN model, by applying Eq. (31). As a specific case, we focus on the body-centered cubic (BCC) HEA, $Mo_{0.2}Nb_{0.2}Ta_{0.2}V_{0.2}W_{0.2}$. We assume that $\zeta_0 \approx b$ and set several of the fundamental alloy properties to averages over those in the component pure metals, i.e., the average Peierls stress is $\sigma_p^0 = 0.586$ GPa and the average shear modulus is $\mu = 90.24$ GPa [35]. Fig. 10 shows the critical stress σ_c as

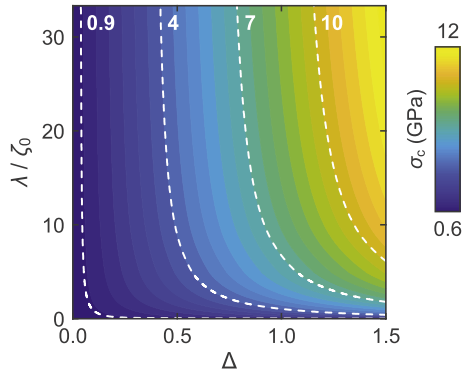

Fig. 10. Critical stress σ_c (Eq. (31)) as a function of the standard deviation Δ and the correlation length λ, which is estimated based on the parameters for BCC $Mo_{0.2}Nb_{0.2}Ta_{0.2}W_{0.2}V_{0.2}$ HEA. The contour lines for several σ_c values are denoted by white dashed lines. The contour line for $\sigma_c = 0.9$ GPa corresponds to the Peierls stress of pure W.

a function of the standard deviation of the amplitude of the generalized stacking-fault energy in the stochastic PN model Δ (see Eq. (31)) and its correlation length λ for this HEA system. In general, σ_c increases with increasing Δ and λ. Fig. 10 shows that for most of the Δ-λ parameter space, the critical stress for the HEA is larger than the Peierls stress of any of the pure metals from which it is formed. This implies that the strength of HEAs will, in general, be higher than those of any of its constituents. Returning to the specific example of $Mo_{0.2}Nb_{0.2}Ta_{0.2}V_{0.2}W_{0.2}$, we assume that the correlation length for the site occupancy is twice the dislocation core size ($\lambda = 2\zeta_0$) and we set Δ to the average Peierls barriers of the five constituent elemental solids ($\Delta = 1.5$), we obtain $\sigma_c = 7.27$ GPa. If we set $\Delta = 1$, we obtain $\sigma_c = 5.04$ GPa. These values should be compared with the average Peierls stress of the five constituent elemental solids, 0.59 GPa, or that of the elemental solid with the largest Peierls stress (i.e., W, 0.9 GPa). This comparison shows that randomness easily provides very large strength increments compared with the HEA constituents. Of course, this is a crude estimate, but makes a strong, clear case.

The finite-temperature, finite-strain-rate yield stress can be estimated from the energy barrier for dislocation glide ΔE_b following common practice [36] as, for example, applied by Varvenne [13]:

$$\sigma(T) = \sigma_c \left[1 - \left(\frac{k_B T}{\Delta E_b} \ln \frac{\dot{\varepsilon}_0}{\dot{\varepsilon}}\right)^{\frac{2}{3}}\right], \tag{32}$$

where σ_c is the critical stress obtained by Eq. (31) and $\dot{\varepsilon}_0$ is a reference strain rate. For most metals, σ_c is usually assumed to be a constant (temperature independent), such that the entire temperature dependence is associated with the term in the square brackets. On the other hand, in HEAs σ_c depends on the compositional correlation length λ. The correlation length depends on the short range order in the material; i.e., λ decreases with increasing T in HEAs [37]. This implies that $\sigma_c(\lambda(T))$ is nearly independent of T at low temperature and very sensitive to T at high temperature; see the dependence of $\overline{\Delta}$ (σ_c is proportional to $\overline{\Delta}$) with respect to λ in Fig. 8. Hence, in HEAs, the temperature dependence of the yield stress is controlled by the term in square brackets in Eq. (32) at low T, but by $\sigma_c(T)$ at high temperature. This implies that the temperature dependence of the yield stress is "normal" at low and intermediate T, but will fall rapidly with increasing T at high T. The is consistent with experimental measurements of the temperature dependence of the yield strength of BCC HEAs [38] (in these experiments, the sample were annealed at the test temperature prior to loading).

In this paper, we incorporated the effects of randomness in HEAs based on the classical PN model [25,26] for undissociated perfect dislocations. For HEAs in which the dislocations do not dissociate into partials, e.g. BCC HEAs, this stochastic PN model applies directly. For FCC HEAs [39,40] in which the two partials are well separated the stochastic PN model can be applied using the approach employed previously in the classical PN model for pure FCC metals [41,42]. While the effects of randomness on the Peierls stress in FCC materials follows the same general description as that for BCC metals discussed here, it is important to keep in mind that the magnitude of the Peierls stress on the strength of FCC metals is much smaller than in BCC metals (the Peierls stress in most pure FCC metals is very small). In FCC metals, the strength is more commonly dominated by dislocation-dislocation interactions and extrinsic strengthening mechanisms; hence, while randomness plays the same role in FCC and BCC alloys its contribution to the overall strength will be significantly smaller in FCC than BCC alloys.

We recall that the main point of this paper is to examine the effect of randomness in HEAs; it clearly does not account for changes in alloy chemistry that change the energy difference between FCC and HCP (which controls stacking fault energy and partial spacing); in fact we note that in some FCC HEAs, the HCP phase may be associated with even lower energy than the FCC phase which suggests a negative stacking fault energy (if the system were equilibrated). Clearly, the effect of changes in the average magnitude of the stacking fault energy is outside the realm of this model.

The stochastic PN model discussed here is based upon several assumptions; we outline the major assumptions here. Many of these assumption could be relaxed via the same approaches employed for the generalization of the elemental PN model. First, our stochastic PN approach is built upon the classical PN model where a nonlinear potential energy across the slip plane is described in terms of a simple cosine function. Of course, more accurate nonlinear potential energy surfaces (the generalized stacking fault energy or γ-surface [43]) may be incorporated (e.g., directly from density functional theory calculations [44–49]). Available techniques for PN models with general γ-surfaces may be applied in the stochastic PN framework; these include, e.g., representing the γ-surfaces by a finite-term Fourier series that reflects the lattice symmetry [47–53], approximate analytical methods [48–50], and solutions based on discrete lattice point models [45,52,54].

Second, unlike our one-dimensional description (where dislocations are edges), dislocations in real materials are not straight and therefore not uniformly edge or screw. Many such curved dislocation PN models have been proposed, e.g., Refs. [51–58]. The difference between edges and screws are important for BCC metals (including HEAs), where there are a predominance of screws. Generalizations of the classical PN model to screw dislocations have been proposed (with partial dissociation in multiple slip planes in BCC lattices) [59,60]; our stochastic PN model can similarly be generalized to include such screw dislocations (with nonplanar cores [61]). We have extended our one-dimensional results to two dimensional slip planes by application of an Orowan pinning model. This, of course, is oversimplified, but may be extended more effectively in two dimensions by considering a two-dimensional inter-planar potential.

8. Conclusions

In this paper, we developed a model to predict the intrinsic yield strength of high-entropy alloys (HEAs) within the framework of the Peierls-Nabarro (PN) model. We assume that the intrinsic yield strength of HEAs is associated with the stress required for dislocation glide; i.e., the Peierls (friction) stress. In the classical PN model, the Peierls stress results from the periodic interplanar potential for dislocation glide in a discrete lattice. In the case of HEAs, we relate the spatial randomness of the composition distribution as stochastic perturbations to the interplanar potential. Accounting for these stochastic perturbations in the PN framework leads to the stochastic PN model developed here.

We developed two versions of the stochastic PN model. The simple version of the stochastic PN model accounts for the randomness in the composition in terms of a distribution of misfit energies, from which we estimate the probability distributions of the dislocation core size, Peierls stress and the distance a dislocation can travel under a particular applied stress. This simple model provides an estimate of the variation of the Peierls stress with respect to the amplitude of the HEA randomness.

Of course, multicomponent alloys must have finite short-range order and hence are not completely random. Our more complete version of the stochastic PN model explicitly considers spatial

correlations within the spatial composition distribution (described here by a Ornstein-Uhlenbeck process); this introduces a spatial correlation parameter. This model gives a Peierls stress that is a function of both the amplitude of the HEA randomness and the correlations within it. From the viewpoint, the simple model should be viewed as one with an infinite correlation length.

The PN model is one dimensional (1D) and can only be directly applied to the case where every point along the dislocation line is in exactly the same (compositional) environment. Of course, a dislocation in an HEA will experience random variations in the composition both as it moves as well as along its length. If there is indeed random composition variations along the dislocation line, the dislocation will not be straight. We extend the 1D stochastic PN model to dislocation glide along its 2D slip plane based on an Orowan approach, where the average spacing between the pinning sites is the probability that an applied stress is larger than the local Peierls stress.

Based upon the stochastic PN model, we see that randomness in the spatial distribution of the composition in HEAs gives rise to a distribution of local Peierls stresses. This distribution of local Peierls stresses implies that dislocations will move by bowing between pinning points (where the local Peierls stress exceeds the applied stress). The net result is that the underlying randomness of an HEA naturally gives rise to an intrinsic yield strength that exceeds that of its constituents. Examples were provided that show that the effective Peierls stress for an HEA exceeds that of any of the constituent single-component metals. The extent of the short range order within the HEA has a strong influence on both its intrinsic yield strength and its temperature dependence. These predictions are consistent with a range of experimental data in BCC HEAs.

Acknowledgements

The authors gratefully acknowledge useful discussions with Prof. Abba Krieger of the Department of Statistics, The University of Pennsylvania. YX acknowledges support of the Hong Kong Research Grants Council General Research Fund 16302818.

Appendix A. Supplementary data

Supplementary data to this article can be found online at https://doi.org/10.1016/j.actamat.2018.12.032.

References

[1] J.-W. Yeh, S.-K. Chen, S.-J. Lin, J.-Y. Gan, T.-S. Chin, T.-T. Shun, C.-H. Tsau, S.-Y. Chang, Nanostructured high-entropy alloys with multiple principal elements: novel alloy design concepts and outcomes, Adv. Eng. Mater. 6 (2004) 299–303.
[2] Y. Zhang, T.T. Zuo, Z. Tang, M. Gao C, K. Dahmen A, P.K. Liaw, Z.P. Lu, Microstructures and properties of high-entropy alloys, Prog. Mater. Sci. 61 (2014) 1–93.
[3] D.B. Miracle, O.N. Senkov, A critical review of high entropy alloys and related concepts, Acta Mater. 122 (2017) 448–511.
[4] A. Gali, E.P. George, Tensile properties of high-and medium-entropy alloys, Intermetallics 39 (2013) 74–78.
[5] B. Gludovatz, A. Hohenwarter, D. Catoor, E.H. Chang, E.P. George, R.O. Ritchie, A fracture-resistant high-entropy alloy for cryogenic applications, Science 345 (2014) 1153–1158.
[6] Y. Shi, B. Yang, P.K. Liaw, Corrosion-resistant high-entropy alloys: a review, Metals 7 (2017) 43.
[7] N.A.P.K. Kumar, C. Li, K.J. Leonard, H. Bei, S.J. Zinkle, Microstructural stability and mechanical behavior of FeNiMnCr high entropy alloy under ion irradiation, Acta Mater. 113 (2016) 230–244.
[8] R. Labusch, A statistical theory of solid solution hardening, Phys. Status Solidi B 41 (1970) 659–669.
[9] O.N. Senkov, J.M. Scott, S.V. Senkova, D.B. Miracle, C.F. Woodward, Microstructure and room temperature properties of a high-entropy TaNbHfZrTi alloy, J. Alloy. Comp. 509 (2011) 6043–6048.
[10] I. Toda-Caraballo, P.E.J. Rivera-Díaz del Castillo, Modelling solid solution hardening in high entropy alloys, Acta Mater. 85 (2015) 14–23.
[11] Z. Wu, Y. Gao, H. Bei, Thermal activation mechanisms and Labusch-type strengthening analysis for a family of high-entropy and equiatomic solid-solution alloys, Acta Mater. 120 (2016) 108–119.
[12] C. Varvenne, A. Luque, W.A. Curtin, Theory of strengthening in fcc high entropy alloys, Acta Mater. 118 (2016) 164–176.
[13] C. Varvenne, G.P.M. Leyson, M. Ghazisaeidi, W.A. Curtin, Solute strengthening in random alloys, Acta Mater. 124 (2017) 660–683.
[14] G.P.M. Leyson, W.A. Curtin, Solute strengthening at high temperatures, Model. Simulat. Mater. Sci. Eng. 24 (2016), 065005.
[15] M.S. Duesbery, V. Vitek, Plastic anisotropy in bcc transition metals, Acta Mater. 46 (1998) 1481–1492.
[16] M.F. Del Grosso, G. Bozzolo, H.O. Mosca, Modeling of high entropy alloys of refractory elements, Physica B 407 (2012) 3285–3287.
[17] P. Singh, A.V. Smirnov, D.D. Johnson, Atomic short-range order and incipient long-range order in high-entropy alloys, Phys. Rev. B 91 (2015) 224204.
[18] A. Tamm, A. Aabloo, M. Klintenberg, M. Stocks, A. Caro, Atomic-scale properties of Ni-based FCC ternary, and quaternary alloys, Acta Mater. 99 (2015) 307–312.
[19] A. Sharma, P. Singh, D.D. Johnson, P.K. Liaw, G. Balasubramanian, Atomistic clustering-ordering and high-strain deformation of an $Al_{0.1}$CrCoFeNi high-entropy alloy, Sci. Rep. 6 (2016) 31028.
[20] F. Körmann, A.V. Ruban, M.H.F. Sluiter, Long-ranged interactions in bcc NbMoTaW high-entropy alloys, Mater. Res. Lett. 5 (2017) 35–40.
[21] J.C. Fisher, On the strength of solid solution alloys, Acta Metall. 2 (1954) 9–10.
[22] M. Jouiad, F. Pettinari, N. Clément, A. Coujou, Dynamic friction stresses in the γ phase of a nickel-based superalloy, Phil. Mag. A 79 (1999) 2591–2602.
[23] F. Pettinari-Sturmel, M. Jouiad, H.O.K. Kirchner, N. Clément, A. Coujou, Local disordering and reordering phenomena induced by mobile dislocations in short-range-ordered solid solutions, Phil. Mag. A 82 (2002) 3045–3054.
[24] F. Otto, A. Dlouhý, C. Somsen, H. Bei, G. Eggeler, E.P. George, The influences of temperature and microstructure on the tensile properties of a CoCrFeMnNi high-entropy alloy, Acta Mater. 61 (2013) 5743–5755.
[25] R. E. Peierls, "The size of a dislocation," Proc. Phys. Soc. 52, 34.
[26] F. R. N. Nabarro, "Dislocations in a simple cubic lattice," Proc. Phys. Soc. 59, 256.
[27] J.P. Hirth, J. Lothe, Theory of Dislocations, second ed., John Wiley, New York, 1982.
[28] J. Frenkel, Zur theorie der elastizitätsgrenze und der festigkeit kristallinischer körper, Z. Phys. 37 (1926) 572–609.
[29] G.E. Uhlenbeck, L.S. Ornstein, On the theory of the brownian motion, Phys. Rev. 36 (1930) 823–841.
[30] M.C. Wang, G.E. Uhlenbeck, On the theory of the brownian motion ii, Rev. Mod. Phys. 17 (1945) 323–342.
[31] J.L. Doob, The brownian movement and stochastic equations, Ann. Math. 43 (1942) 351–369.
[32] I. Karatzas, S.E. Shreve, Brownian Motion and Stochastic Calculus, Springer-Verlag, 1988.
[33] E. Orowan, Symposium on internal stress in metals and alloys, Metals and Alloys (1948) 451.
[34] R.L. Fleischer, Substitutional solution hardening, Acta Metall. 11 (1963) 203–209.
[35] L. Dezerald, L. Ventelon, E. Clouet, C. Denoual, D. Rodney, F. Willaime, Ab initio modeling of the two-dimensional energy landscape of screw dislocations in bcc transition metals, Phys. Rev. B 89 (2014), 024104.
[36] A. Argon, Strengthening Mechanisms in Crystal Plasticity, Oxford University Press, 2008.
[37] A. Fernández-Caballero, J.S. Wróbel, P.M. Mummery, D. Nguyen-Manh, Short-range order in high entropy alloys: theoretical formulation and application to Mo-Nb-Ta-V-W system, J. Phase Equilibria Diffusion 38 (2017) 391–403.
[38] O.N. Senkov, G.B. Wilks, J.M. Scott, D.B. Miracle, Mechanical properties of $Nb_{25}Mo_{25}Ta_{25}W_{25}$ and $V_{20}Nb_{20}Mo_{20}Ta_{20}W_{20}$ refractory high entropy alloys, Intermetallics 19 (2011) 698–706.
[39] A.J. Zaddach, C. Niu, C.C. Koch, D.L. Irving, Mechanical properties and stacking fault energies of NiFeCrCoMn high-entropy alloy, J. Occup. Med. 65 (2013) 1780–1789.
[40] S. Huang, W. Li, S. Lu, F. Tian, J. Shen, E. Holmström, Temperature dependent stacking fault energy of FeCrCoNiMn high entropy alloy, Scripta Mater. 108 (2015) 44–47.
[41] F.R.N. Nabarro, Theoretical and experimental estimates of the peierls stress, Philos. Mag. A 75 (1997) 703–711.
[42] G. Schoeck, The peierls stress and the flow stress in fcc metals, Scripta Metall. Mater. 30 (1994) 611–613.
[43] V. Vitek, Intrinsic stacking faults in body-centred cubic crystals, Philos. Mag. 18 (1968) 773–786.
[44] E. Kaxiras, M.S. Duesbery, Free energies of generalized stacking faults in Si and implications for the brittle-ductile transition, Phys. Rev. Lett. 70 (1993) 3752–3755.
[45] V.V. Bulatov, E. Kaxiras, Semidiscrete variational Peierls framework for dislocation core properties, Phys. Rev. Lett. 78 (1997) 4221–4223.
[46] G. Lu, N. Kioussis, V.V. Bulatov, E. Kaxiras, Generalized stacking fault energy surface and dislocation properties of aluminum, Phys. Rev. B 62 (2000) 3099–3108.
[47] S. Zhou, J. Han, S. Dai, J. Sun, D.J. Srolovitz, van der Waals bilayer energetics: generalized stacking-fault energy of graphene, boron nitride, and graphene/boron nitride bilayers, Phys. Rev. B 92 (2015) 155438.

[48] Z. Pei, M. Eisenbach, Acceleration of the Particle Swarm Optimization for Peierls-Nabarro modeling of dislocations in conventional and high-entropy alloys, Comput. Phys. Commun. 215 (2017) 7–12.
[49] Z. Pei, G.M. Stocks, Origin of the sensitivity in modeling the glide behaviour of dislocations, Int. J. Plast. 106 (2018) 48–56.
[50] G. Schoeck, The Peierls model: progress and limitations, Mat. Sci. Eng. A 400–401 (2005) 7–17.
[51] Y. Xiang, H. Wei, P.B. Ming, W. E, A generalized Peierls–Nabarro model for curved dislocations and core structures of dislocation loops in Al and Cu, Acta Mater. 56 (2008) 1447–1460.
[52] H. Wei, Y. Xiang, "A generalized Peierls–Nabarro model for kinked dislocations, Philos. Mag. 89 (2009) 2333–2354.
[53] S. Dai, Y. Xiang, D.J. Srolovitz, Structure and energy of (111) low-angle twist boundaries in Al, Cu and Ni, Acta Mater. 61 (2013) 1327–1337.
[54] C. Shen, J. Li, Y. Wang, Predicting structure and energy of dislocations and grain boundaries, Acta Mater. 74 (2014) 125–131.
[55] G. Xu, A.S. Argon, Homogeneous nucleation of dislocation loops under stress in perfect crystals, Phil. Mag. Lett. 80 (2000) 605–611.
[56] M. Koslowski, A.M. Cuitino, M. Ortiz, A phase-field theory of dislocation dynamics, strain hardening and hysteresis in ductile single crystals, J. Mech. Phys. Solid. 50 (2002) 2597–2635.
[57] C. Shen, Y. Wang, Incorporation of γ-surface to phase field model of dislocations: simulating dislocation dissociation in fcc crystals, Acta Mater. 52 (2004) 683–691.
[58] J.R. Mianroodi, B. Svendsen, Atomistically determined phase-field modeling of dislocation dissociation, stacking fault formation, dislocation slip, and reactions in fcc systems, J. Mech. Phys. Solid. 77 (2015) 109–122.
[59] M.S. Duesbery, V. Vtek, D.K. Bowen, The effect of shear stress on the screw dislocation core structure in body-centred cubiclattices, Proc. Roy. Soc. Lond. A 332 (1973) 85–111.
[60] A.H.W. Ngan, A generalized Peierls-Nabarro model for nonplanar screw dislocation cores, J. Mech. Phys. Solid. 45 (1997) 903–921.
[61] S.I. Rao, C. Varvenne, C. Woodward, T.A. Parthasarathy, D. Miracle, O.N. Senkov, W.A. Curtin, Atomistic simulations of dislocations in a model bcc multicomponent concentrated solid solution alloy, Acta Mater. 125 (2017) 311–320.